

# Check 23. Journal IREACO Scopus Human ear recognition methods based on image rotation.pdf

*by* Arta Moro Sundjaja

---

**Submission date:** 06-Nov-2018 09:49AM (UTC+0700)

**Submission ID:** 624024364

**File name:** Scopus\_Human\_ear\_recognition\_methods\_based\_on\_image\_rotation.pdf (716.08K)

**Word count:** 6240

**Character count:** 31403

## Human Ear Recognition Methods Based on Image Rotation

Suharjito, Alpha Epsilon, Abba Suganda Girsang

**Abstract** – The ear is part of biometrics that has a unique and stable structure, avoided from aging. This study aims to look at the accuracy of Geometric Moment invariant (GMI) and Zernike Moment invariant (ZMI) with Self-Organizing Maps to recognize human ears. This study used data from ear AMI database, consisting of 125 ears from 25 different people, in which each person has 5 images of the right ear. In this study, each image of the ear is modified with a different rotation angle. The accuracy of ear image recognition using GMI is 75.20% while using ZMI is 66%. The accuracy of using Geometric Moment Invariant is higher by 9.2% because Geometric Moment Invariant does not change the result of the image to be recognized due to translation, scaling, reflection and rotation. GMI cannot recognize the image of the ear with an average of 24.80% while the ZMI cannot recognize the image of the ear with an average of 34.40%. From the test results, at a rotation angle of 30 ° CCW, the geometric moment method has the best accuracy, while the Zernike moment method has the best accuracy at 30 ° CW. The best angle recognized by these two methods is 30°. Copyright © 2017 Praise Worthy Prize S.r.l. - All rights reserved.

**Keywords:** Ear Recognition, Geometric Moment Invariant, Zernike Moment Invariant, Self-Organizing Maps

### Nomenclature

CCW	Counterclockwise
CW	Clockwise
DNA	Deoxyribonucleic acid
GMI	Geometric Moment invariant
$m_{pq}$	Value image of geometric moment in two dimension $p$ and $q$ where $p, q = 0, 1, 2, \dots$
PIN	Personal identity number
SOM	Self Organizing Maps
$x, y$	Coordinant images in geometric moment
$\bar{x}, \bar{y}$	Intensity moment
$\mu_{pq}$	Central moment in dimension $p$ and $q$
$\eta_{pq}$	Normalizing moment in dimension $p$ and $q$
$\phi_1$ to $\phi_7$	Value geometric moment 1 to 7
$ZM_1 - ZM_6$	Zernika moments index 1 to 6

### I. Introduction

Human recognition has become an important issue in social media. In general, traditional identification methods such as entering a PIN, username, and password to log in and display an identification card in a commercial system have some disadvantages in that users must actively participate in the identification process.

It is difficult to remember PIN. Also, the PIN can be easily guessed. Biometric methods can deal with the above problems significantly, because users are identified

by who they are, not with something to remember or carry [1]. Biometric identification methods have been proved to be very efficient, more natural and easier for users than traditional methods of human identification. In fact, biometric method is the only method that actually identifies humans. In recent years, biometric has received a lot of attention [2]. A biometric method of pattern recognition can identify a person by determining the authenticity of a specific physiological characteristic owned by the person. Some commonly used biometrics are DNA, ear, fingerprint, iris, retina, voice and face [3]. Ear recognition is unique and stable. Thus, it reduces the possibility of damage to the equipment when compared with fingerprint recognition [4].

Ear structure does not change proportionally as the increase of age [5] and is not affected by expression and health. However, ear recognition still faces many problems such as occlusion and lighting [6]. Some advantages of using ear as a source of data for personal identification are: ear does not change much over human life, and face changing is more significant within years, than any other parts of human body. Face can also be changed because of cosmetics and hair care. Second, face can be easily changed due to emotions changes and states of mind such as sadness, happiness, or surprise. Instead, ear is relatively fixed and unchanging [1]. Ear is a relatively new class in biometrics. Ear feature has been used for many years in forensic science for recognition. Ear possesses all the characteristics of biometric properties (uniqueness, universality, permanence and collectibility). Ears do not have a random structure.

Unlike human face, ears do not have any change of expression and have a constant color [4]. A study by [6] that had done ear recognition by using  $4 \times 4$  ear images provides the highest accuracy, that is 62.5%. Meanwhile, a study by [7] proposed SOM method to identify a person's ear by calculating the geometric distance of ear image using 138 images data taken for 23 people. This study obtained an identification accuracy of 98%, proving that there is only one misidentification due to good clustering so that all similar data are grouped into one. If we use SOM method for crimes identification, it will be considered very strong and the system is reliable [7]. Meanwhile, a study by [4] using Zernike moment to normalize the image has an accuracy of 94.4%. The method can effectively reduce the discretization error by improving the differentiation of functions of the image but it took a long time because of the amount of training data and the iterative process performed [8]. Based on the description above, this study focuses on ear recognition by comparing the Geometric Moment Invariant (GMI) and Zernike Moment invariant (ZMI) as feature extraction with Self Organizing Maps (SOM) algorithm for clustering. The accuracy results of each method by [7] and [8] are not much different. It is because the different parameters used in the tests were performed as different data sources; many different data were viewed from the lighting and the size of the data used, and there were many different iterations for training in each method. Therefore, it is difficult to determine which method is better (superior) in recognizing ears. It can be seen that the advantages of the ZMI are that the standard method and it works well, and that its implementation is simple, using only 6 moment values. However, the process is slow due to the rotation of continuous iterations that make it harder to get the exact time of training. Meanwhile, the advantage of GMI with SOM is that the results are more accurate and unsupervised in order to perform the mapping by itself. However, it also has an advantage; the length of the recognition process and the results determined by its high-low learning rate with the use of 7 moment values is better than ZMI.

Based on the above study, a comparison of the two methods will be done, particularly to identify the advantages and disadvantages of each method including the level of accuracy and performance of the recognition of human ear with GMI method, and ZMI with Self Organizing Maps by using a sample of the same data, the amount of the same data, and the same parameters, resulting in accurate comparison results.

## II. Related Works

Research by [9] employed a data sample of 17 people as experiment subjects with six images from each person. The data used were obtained from the National Institute of Standards and Technology (NIST). Correct recognition rate ranged between 84.3% and 91.2% for neural network matching. It depends on the neural network training parameters. Meanwhile, a study by

[7] on the use of SOM has been proposed for identifying a person's ear by calculating the geometric distance of ear images using 138 image data taken for 23 people. This study obtained 98% identification accuracy, proved that there is only one fault identification that can be used for crime identification because this method can create reliable and very accurate systems. The next is a study by [5] on ear recognition using back propagation neural network with 350 sets of training data, and 150 test data. This study obtained 98% accuracy. The disadvantage is that the data set used did not employ a trusted ear database.

Research by [8] used Zernike moment to normalize the image of the input data which consists of 36 images of the alphabet and numbers with the written form of capital Times New Roman sized 72 extracted using Zernike moments and classification Nearest Neighbor (NN). [8] tested the performance of Zernike moment descriptor, NN classification included to recognize the gray level images of 26 capital letters and 10 digits. The results showed that the level of accuracy was 86.4% of letters and numbers that are recognized. Then, using Zernike moment, the level of recognition accuracy increased to 94.4%. This study concluded that the accuracy of the normalization of Zernike moment's image can be quite effective. Research by [10] using Log Gabor Filter feature extraction has 92.66% accuracy rate by using 150 ear images under a variety of different lighting conditions. Research by [11] used geometric features, which generate seven invariant values used as the feature vector of the ear image producing 98% accuracy by increasing the distance taken to improve the vectors in the image so that it will be more representative. This process will be discussed in the methodology section.

## III. Methodology

In the implementation of Geometric Moment invariant method and SOM, and Zernik Moment invariant and SOM for the human ear recognition system, the computer system is not equipped with 'the way of thinking' like a human; that is why the computer must go through several stages to recognize ear images. Here are the analysis stages of ear recognition problems.

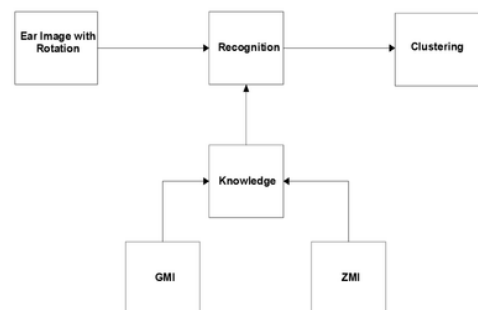


Fig. 1. Ear Recognition Flow Process

Starting from searching data of human ear images to be inputs to the system; then, the pre-processing and extraction are done using GMI and ZMI that will generate knowledge.

The next step is ear recognition by grouping images using SOM. Fig. 2 shows the framework of this study. The stages of the research will be discussed in the next section, which are illustrated by an image to indicate the general stages conducted in this research.

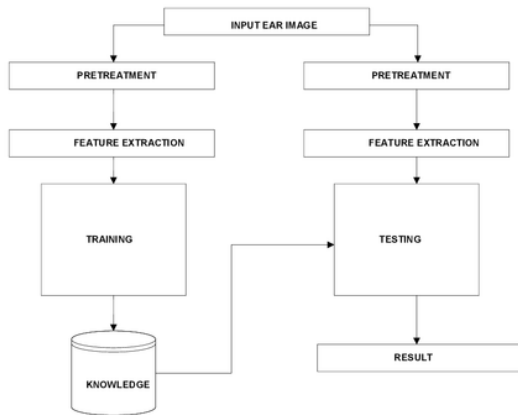


Fig. 2. Ear Recognition Framework

The image of the ear used secondary data, the secondary data or data derived from the database of 25 people who have not been modified using rotations obtained from the internet already having the criteria of AMI database ear ([http://www.ctim.es/research\\_works/ami\\_ear\\_database/](http://www.ctim.es/research_works/ami_ear_database/)) with a resolution of  $115 \times 175$ . Data for each person consist of 3 models of the image of the right ear per person for a position taken in a vertical differentiated image with three models making positions, where the image was taken with the ears slightly downward position, facing straight ahead, and taking a little left. Then, the rotation angle of the 3 ear images is modified so that 1 image of ear will produce 5 images after the modification of angles, using the following angles of rotation  $0^\circ$ ,  $15^\circ$  CW (Clockwise),  $30^\circ$  CW (Clockwise),  $15^\circ$  CCW (CounterClockwise),  $30^\circ$  CW (CounterClockwise).

From the results of this modification, 375 ear images are obtained, which will be used as input data for this study. The data are used later to do ear training, which is the model image with the image acquisition facing straight ahead and slightly left, and the data that will be used for testing using a model of the image of the ear facing slightly downward. For image pretreatment described in section 3 models, Fig. 3 shows the image of the ear that comes from AMI database.

### III.1. Research Flow Chart

This section describes the flowchart of concepts that will be carried out in the research.

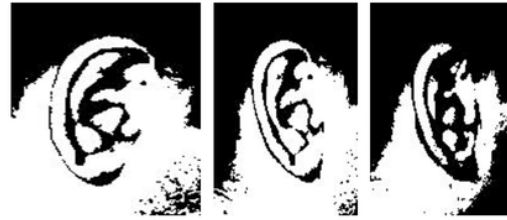


Fig. 3. The image data from the AMI database ears

From the flowchart indicated in Fig. 4, it can be seen that in the initial process, user inputs the primary / secondary ear images and then the system will process the images for the pre-processing (each image is converted into a thresholding). Furthermore, the user selects which feature extraction that will be used, whether the ZMI or GMI method. By using the ZMI method, the feature extraction will be correcting the best weights to be entered into the test to produce ear image accuracy. However, if the user chooses GMI method, the system will perform data clustering using SOM in order to get ear image recognition accuracy.

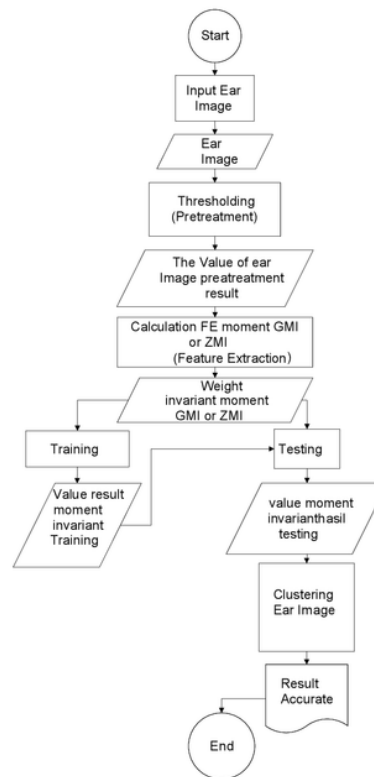


Fig. 4. Research Stages Flowchart

Ear images will be heading to the pre-processing stage to make changes to the resolution, grayscale, and threshold. Preprocessing stages use Adobe Photoshop



CS4 software. First, primary and secondary ear image data are still in the form of RGB color image which will be inserted to a worksheet using Photoshop. Then, the images are converted into grayscale images. Grayscale image process is done in order to perform a threshold process. Furthermore, ear image color will be converted into black and white. Fig. 5 shows the stages of preprocessing using Photoshop.



Fig. 5. Preprocessing by Using Photoshop CS4

Fig. 5 is a preprocessing stage when the resolution change is done. Then, the RGB image will be converted to a grayscale image, for later to be converted into threshold image. The next step, the pre-processing step is repeated, which will be using ear recognition software to search ear image edge with Sobels.



Fig. 6. Preprocessing with Ear Recognition Software

Ear images that have been processed into a threshold will be pre-processed to obtain image edge with Sobel detection included in gradient edge detector where Sobel detects the maximum and minimum values of the edges of ear images in order to get the boundaries of the ear images, and to obtain clearer information data. The detection limit (edge) of an image uses the Sobel  $3 \times 3$  matrix with coefficients that have been determined as follows (Fig. 7).

-1	0	+1	+1	+2	+1
-2	0	+2	0	0	0
-1	0	+1	-1	-2	-1
Gx			Gy		

Fig. 7. Sobel Matrix

### III.2. Feature Extraction using Geometric Moment Invariant

Geometric Moment invariant feature extraction is used to obtain pixel values. Pixels containing the value are used to obtain a special feature of the ear images. Geometric Moment invariant has seven features that do not change the translation value, change of scale, mirroring and rotation [12].

Step-by-step calculations of geometric moments are described as follows:

- 1) Read the input image data from left to right and from top to bottom.
- 2) Image is converted into threshold to extract the target process area.
- 3) Calculate the value of the image,  $m_{pq}$  using:

$$m_{pq} = \sum_x \sum_y x^p y^q f(x, y) \quad (1)$$

Description:

$m_{pq}$ : Two dimension moments.

p and q: Integer 0, 1, 2, 3, ...,

x, y: Image coordinates,

$x^p y^q$ : Function based.

- 4) Calculate the intensity moment  $(\bar{x}, \bar{y})$  by using:

$$\bar{x} = \frac{m_{10}}{m_{00}} \text{ and } \bar{y} = \frac{m_{01}}{m_{00}} \quad (2)$$

- 5) Calculate central moment,  $\mu_{pq}$  by using:

$$\mu_{pq} = \sum_{x=0}^{M-1} \sum_{y=0}^{N-1} (x - \bar{x})^p \cdot (y - \bar{y})^q f(x, y) \quad (3)$$

- 6) Normalizing moment,  $\eta_{pq}$  to be used in image scale by using:

$$\gamma = \frac{p+q+2}{2}, \eta_{pq} = \frac{\mu_{pq}}{\mu_{00}^\gamma}, \quad p, q = 2, 3, \dots \quad (4)$$

- 7) Calculate the geometric moment,  $\varphi_1$  to  $\varphi_7$  to translation, scaling and rotation invariant (invariant Geometric Moments) using the following formula:

$$\varphi_1 = \eta_{20} + \eta_{02} \quad (5)$$

$$\varphi_2 = (\eta_{20} - \eta_{02})^2 + 4\eta_{11}^2 \quad (6)$$

$$\varphi_3 = (\eta_{30} - 3\eta_{12})^2 + (\eta_{03} - \eta_{21})^2 \quad (7)$$

$$\varphi_4 = (\eta_{30} + \eta_{12})^2 + (\eta_{03} + \eta_{21})^2 \quad (8)$$

$$\varphi_5 = (\eta_{30} - 3\eta_{12})(\eta_{30} + \eta_{12})\{(\eta_{30} - 3\eta_{12})^2 - 3(\eta_{21} + \eta_{03})^2\} + (3\eta_{21} - \eta_{03})(\eta_{21} + \eta_{03})\{3(\eta_{30} + \eta_{12})^2 - (\eta_{21} + \eta_{03})^2\} \quad (9)$$

$$\varphi_6 = (\eta_{20} - \eta_{02})\{(\eta_{30} + \eta_{12})^2 - (\eta_{21} + \eta_{03})^2\} + 4\eta_{11}(\eta_{30} + \eta_{12})(\eta_{21} + \eta_{03}) \quad (10)$$

$$\varphi_7 = (3\eta_{21} - \eta_{03})(\eta_{30} + \eta_{12})\{(\eta_{30} + \eta_{12})^2 - 3(\eta_{21} + \eta_{03})^2\} + (3\eta_{21} - \eta_{03})(\eta_{21} + \eta_{03})\{3(\eta_{30} + \eta_{12})^2 - (\eta_{21} + \eta_{03})^2\} \quad (11)$$

The numerical value calculated from  $\varphi_1$  to  $\varphi_7$  is very small. So, the absolute logarithm value from the function can be used as a feature to represent the

image. Based on the explanation from the equation that has been made above, a Geometric Moment invariant process can be designed as shown in Fig. 8.

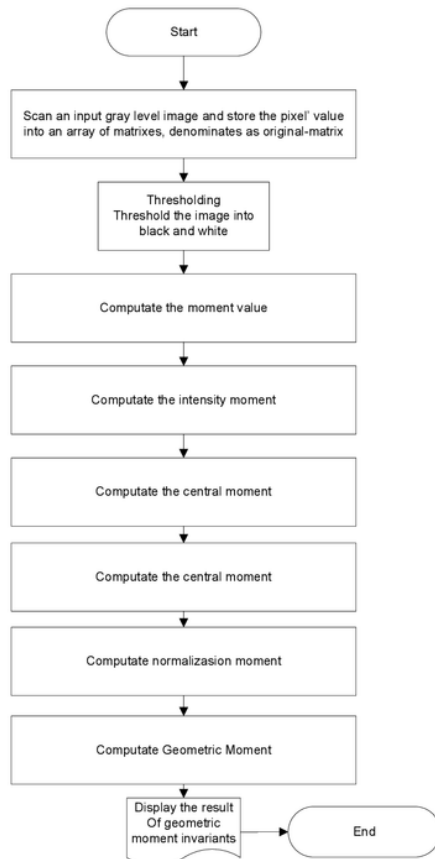


Fig. 8. Illustration Process of Geometric Moment Invariants Flow Chart [13]

### III.3. Feature Extraction Using Zernike Moment Invariant

Zernike moment was first introduced by Teague [14]. In terms of calculation, Zernike moment involves more complex calculation than other types such as geometric moment and Legendre moment. However, Zernike moment has been proven as one of good feature extraction methods because of its ability to present a distorted image and rotation [15].

Zernike moment is included in region-based shape descriptor. This type of moment is known to be very efficient in its use for pattern recognition because it has an orthogonality characteristic on Zernike polynomials in feature extraction results that has been formed and has a characteristic that does not depend on the rotation of the image. Central moment (p, q) which has been normalized is defined as:

$$\eta_{pq} = \frac{\mu_{pq}}{(\mu_{00})^{\frac{p+q+2}{2}}} \quad (12)$$

[16] uses six equations on Zernike moments:

$$ZM_1 = \frac{3}{\pi} [2(\eta_{20} + \eta_{02} - 1)] \quad (13)$$

$$ZM_2 = \frac{9}{\pi^2} [(\eta_{20} - \eta_{02})^2 + 4\eta_{11}^2] \quad (14)$$

$$ZM_3 = \frac{16}{\pi^2} [(\eta_{03} - 3\eta_{21})^2 + (\eta_{30} - 3\eta_{12})^2] \quad (15)$$

$$ZM_4 = \frac{144}{\pi^2} [(\eta_{03} - 3\eta_{21})^2 + (\eta_{30} + \eta_{12})^2] \quad (16)$$

$$ZM_5 = \frac{13824}{\pi^4} \left\{ \begin{array}{l} (\eta_{03} - 3\eta_{21})(\eta_{03} + \eta_{21}) \\ [(\eta_{03} + \eta_{21})^2 - 3(\eta_{30} + \eta_{12})^2] \\ - (\eta_{30} - 3\eta_{12})(\eta_{30} + \eta_{12}) \\ [(\eta_{30} + \eta_{12})^2 - 3(\eta_{03} + \eta_{21})^2] \end{array} \right\} \quad (17)$$

$$ZM_6 = \frac{864}{\pi^3} \left\{ \begin{array}{l} (\eta_{02} - \eta_{20}) \left[ \frac{(\eta_{30} + \eta_{12})^2}{4\eta_{11}(\eta_{03} + \eta_{21})(\eta_{30} + \eta_{12})} \right] + \end{array} \right\} \quad (18)$$

### III.4. Self Organizing Maps (SOM) Algorithm

Grouping is an unsupervised learning, because it is associated with finding the structure in the labeled data set. Another definition of clustering could be a "process of organizing objects into groups which have similar members in some ways." A cluster is a collection of objects that are "similar" among them and "different" from an object belonging to another group [17].

Kohonen [18] has adopted SOM for grouping data without knowing the class of membership of input data and it has been very successful in a pattern recognition field (such as handwriting recognition and ear recognition) (Bullinaria, 2004). SOM is an unsupervised system based on competitive learning, where each output neuron competes and has a winner neuron which can be updated later [19].

## IV. Results and Discussions

### IV.1. Image Preparation Process

Referring to the source database ear AMI database ([http://www.ctim.es/research\\_works/ami\\_ear\\_database/](http://www.ctim.es/research_works/ami_ear_database/)), the processes of image preparation require some things. First, the execution of modifications to the rotation of 0 degrees, 15 degrees CW (Clockwise), 30 degrees CW (Clockwise), 15 degrees CCW (counterclockwise), 30 degrees CCW (counterclockwise) with the aim of preparing the image made to produce images with good quality. Image preparation process is performed before the process of feature extraction and clustering. All images used prior to

the preparation process has a color RGB image. Preparation process of the image includes the transformation process of a color image to grayscale (Grayscale), and thresholding and edge detection process (edge detection). For pretreatment, the image analysis is described in pretreatment section. The examples of images with a new rotation are shown in Fig. 9.



Fig. 9. Examples of image rotation Ear After modification process in which the initial position of 0 degrees, and changed to 15 degrees CW (Clockwise), 30 degrees CW (Clockwise), 15 degrees CCW (counterclockwise), 30 CCW (counterclockwise)

#### IV.2. Transformation Process of Color Images

The transformation process colors used are gray level image (grayscale), which is an image processing by changing the values of the initial image pixels into an image of gray. This transformation aims to improve the contrast of the image, so that the information on that image can be seen. A gray image is an image that uses only gray color levels. Gray level here is gray with various levels of black to nearly white. Gray color is the only color in RGB space with components of red, green, and blue with the same intensity. This image at each pixel contains a layer where the value is in the interval 0-255 intensity, so that the pixel values in the gray image can be represented in a matrix that can facilitate the process of calculating the next operation. The images obtained from the dataset ear Ear AMI database are images created with the RGB color model which has 3 channels. In this process, each pixel in the third canal system is transformed into shades of gray. The transformation processes color system of RGB color system into a system of gray mathematically; the calculation of gray image can be formulated by Equation (19):

$$S = \frac{R + G + B}{3} \quad (19)$$

$S$  expresses degrees of gray;  $R$  represents the value of intensity of red (red);  $G$  states value of the intensity of the green color (green), and  $B$  represents the value of the intensity of blue color (blue).

#### IV.3. Thresholding Process

Thresholding is a process to produce a binary image (bilevel) of the image of gray. Bilevel image is the image having gray levels in two classes which are black and white, from 0 for black and one for white. Grouping bilevel image pixel by pixel can be zoomed and facilitates the operation of the process of some images as

form recognition and classification. In a simple implementation, the output of the thresholding operation is a binary image. An overall value of bilevel shows the results that can be classified into black and white. At the time of displaying the image, 0 is white and one is black.

This process aims to change the image of the gray color system into a system image with black-and-white (binary).

#### IV.4. Edge Detection Process

The process of edge detection (Edge Detection) is applied to the binary image and is a process that changes the morphology of the image which is the image that contains only the edge / line the periphery of the ear. Example ear edge detection process results are shown as follows:



Fig. 10. Example Ear edge detection process results

#### IV.5. Research Result

Tests conducted in this study are the result of testing GMI feature extraction and feature extraction ZMI later in clustering using SOM.

Ear image data used for training include 250 data and testing with data from 125 different models. Testing is done by entering the entire image of the right ear tested on the system to find out the results of the rank of recognition accuracy. The comparison of ear recognition results with feature extraction of ZMI and GMI using Clustering SOM is presented in Fig. 11.

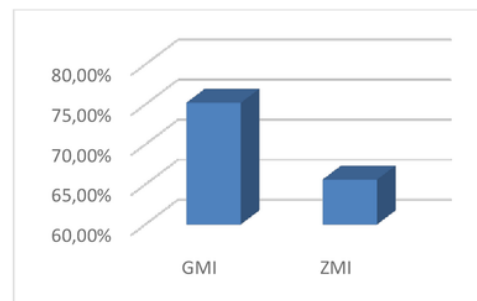


Fig. 11. Comparison of ear images recognized by GMI and ZMI

As shown in Fig. 11 feature extraction using GMI in ear recognition can recognize 94 ear images or as much as 75.20% recognized ear images, whereas ZMI recognizes only 84 ear images or 66% recognized ear images of total data testing of 125 ear images.



From the above comparison results, an image analysis was performed with any angle that causes GMI and ZMI to be able to recognize the ear well. The comparison of ear recognition results using ZMI and GMI with various rotation angles is explained in Table I.

TABLE I  
THE PERFORMANCE COMPARISON OF GMI AND ZMI RECOGNIZES EAR FOR DIFFERENT ANGLES OF ROTATION

No	Method	0°	15° CW	15° CCW	30° CW	30° CCW	Total & % Average
1	GMI	15	17	17	21	24	94
	%	60%	68%	68%	84%	96%	75.20%
2	ZMI	9	16	14	24	19	82
	%	36%	64%	56%	96%	76%	65.60%

Based on Table I, it appears that ZMI and GMI can recognize ear images at an angle of 30° CW with the highest and lowest values recognizing the ear image being tied at an angle of 0°. GMI and ZMI methods can recognize the ear image well at 30° CW rotation angle with 96% ear recognition rate by ZMI and 84% by GMI. Meanwhile, on average for each rotation angle, ear recognition rate with GMI method is better than the rate of image recognition using ZMI method that is 75.2% and 65.6% respectively. This suggests that the GMI method is more stable in recognizing the ear image for angular change than the ZMI method, although the ear recognition of ZMI method is higher than the GMI method at the rotation angle of 30° CW.

As shown in Fig. 12, the number of ear images recognized by the GMI method is greater than the number of images recognized by the ZMI method for various rotational angles, except at the rotation angle of 30° CW which shows that the number of ear images recognized by ZMI is greater than the number of ear images recognized by GMI.

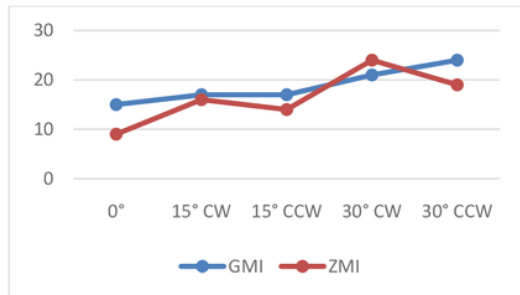


Fig. 12. Comparison of the number of ear images that GMI and ZMI recognize for different angles

Based on Fig. 12 and Fig. 13, the comparison of ear recognition performance with GMI and ZMI for different angles of rotation seen GMI looks to have better ear image recognition performance compared to ZMI for various rotation angles. This is shown by the average value obtained on the GMI method that can recognize the ear image with an average of 75.20% while the ZMI method only recognizes the ear image with an average of 66%. From the comparison above, an analysis of the

image is done by any angle that causes GMI and ZMI does not recognize the image of the ear; the analysis is as follows.

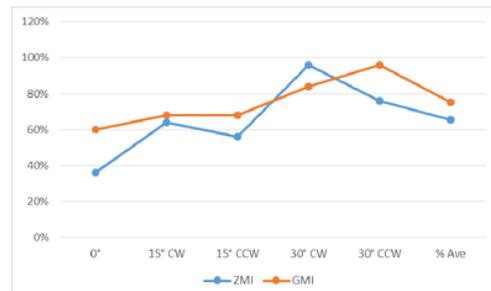


Fig. 13. Comparison of ear recognition percentage with GMI and ZMI for various angle of rotation

TABLE II  
THE PERFORMANCE COMPARISON OF GMI AND ZMI DOES NOT RECOGNIZE EAR FOR DIFFERENT ANGLES OF ROTATION

No	Method	0°	15° CW	15° CCW	30° CW	30° CCW	Average %
1	GMI	10	8	8	4	1	31
	%	40%	32%	32%	16%	4%	24.80%
2	ZMI	16	9	11	1	6	31
	%	64%	36%	44%	4%	24%	34.40%

Table II is used to explain the failure of GMI and ZMI methods in recognizing ear images by rotation angles. Based on the table, along with the increasing angle of rotation, the failure rate of recognition of ear image decreased for both of these methods. These results indicate that the rate of failure of ear image recognition by ZMI and GMI methods can be decreased by increasing the angle of rotation.

The results of the comparison of ear image recognition on GMI and ZMI methods are explained in Fig. 14. From the figure, it can be seen that the failure rate of ear image recognition on the GMI method is always lower than the ZMI method for each rotation angle except at the rotation angle of 30° CW. Variations in the number of ear images that cannot be recognized by the ZMI method are higher than the variations in the number of images that the GMI method cannot recognize.

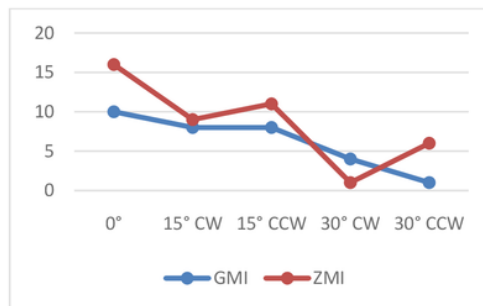


Fig. 14. Comparison of the number of ear images that can not be recognized by GMI and ZMI methods



These results indicate that the GMI method is more stable than the ZMI method for recognizing the ear image with rotational angle changes.

As shown in Fig. 15, the ZMI method has a higher percentage than the GMI method in terms of failure to recognize ear images at different rotation angles, except at an angle of 30° CW when the percentage value of the ZMI method is lower than the percentage value of the GMI method. The average percentage of ear image recognition failure of ZMI method is 34.40% while the mean failure rate of ear image recognition of GMI method is 24.80%. These results indicate that the GMI method is better than the ZMI method for recognizing the ear image in multiple rotation angles.

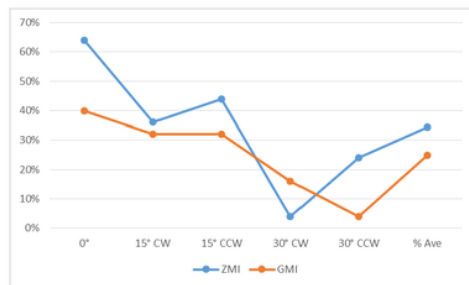


Fig. 15. Comparison of percentage of ear image that can not be recognized by GMI and ZMI methods

Test results using 250 training data and 125 testing data from ear image with different rotation angle indicate that the use of GMI feature extraction method in ear image recognition has an accuracy level of 75.20%. Meanwhile, the use of ZMI feature extraction method in the ear image recognition has an accuracy level of 66%. From this comparison, they appear to be different because feature extraction from the GMI method has more features than the ZMI method. So, GMI method can recognize a more detailed biometric object. This is a technique that does not change the feature extraction results generated by the translations, scaling, reflection and rotation of the image to be recognized. ZMI feature extraction method is more suitable for recognizing rigid objects such as numbers and letters because ZMI is very efficient to perform feature extraction on image recognition that has a certain pattern.

From the above test, it can also be seen that GMI is able to recognize the image of the ear with many conditions different angles looks GMI can recognize the angle of the image of the ears of 0° as many as 15 images ear recognizable, to the data 15° CW GMI can recognize as many as 17 images ear, to the data 30° CW can recognize as many as 21 images ear, and at an angle of 30° CCW GMI 24 can recognize the image of the ears of 25 images per angular ears. While ZMI can only recognize the corner of the image of the ears of 0° as much as 9 image ear recognizable, to the data 15° CW ZMI can recognize as many as 16 images ear, to the data 30° CW can recognize as many as 24 images ear, and at

an angle of 30° CCW GMI can recognize the image 19 ears of 25 images per angular ears. Judging from the comparison of the average angle of unrecognized ZMI cannot recognize the image of an ear with an average of 34.40%, while GMI simply cannot recognize the image of an ear with an average of 24.80% making it more visible if ZMI is difficult to recognize the image of the ear with multiple angles rotation.

## V. Conclusions and Suggestions

Based on the results of this research, some conclusions can be drawn: The software created using GMI and SOM has a high accuracy rate when compared to the software using ZMI and SOM.

Based on analysis of the experimental results, ear recognition accuracy with secondary data using GMI and SOM is 91.20% and using the ZMI and SOM is 88.80%. The objectives of this research has been reached to see a comparison of methods using GMI feature extraction and SOM clustering method and using the ZMI feature extraction and SOM clustering, as well as biometrics ear recognition using GMI and SOM clustering is better because it has more invariants calculation which is compared to ZMI that has less calculations and recognition using ZMI is more suitable for recognition that has more firmer object structure image as literacy and numeracy.

GMI can recognize the image of the ear angle 0° as many as 15 images are recognizable ear, to the data 15° CW GMI can recognize as many as 17 images ear, to the data 30° CW can recognize as many as 21 images ear, and at an angle of 30° CCW can GMI 24 recognize the image of the ear of the ear image 25 from an angle. While ZMI can only recognize the corner of the image of the ears of 0° as much as 9 image ear recognized, to the data 15° CW ZMI can recognize as many as 16 images ear, to the data 30° CW can recognize as many as 24 images ear, and at an angle of 30° CCW GMI can recognize image 19 ears of 25 images per angular ears. Seen that GMI simply cannot recognize the image of an ear with an average of 24.80% while the ZMI cannot recognize the image of an ear with an average of 34.40% so that GMI is better used for identification purposes that are not affected due to the geometric rotation.

Suggestions for the further development of this study are as follows: Inserting a pre-processing process into the system to get a better ear structures; Comparing the results of images with JPEG format with other formats such as BMP, PNG, etc; Distinguishing data processed by race / ethnicity in order to be more specified; This study is still a prototype that can be implemented into a larger system to make the system work in realtime, such as: System Security and Surveillance System.

## Acknowledgements

This work was supported by Bina Nusantara University.

## References

- [1] M. Choraś, "Ear biometrics based on geometrical feature extraction," *Progress in Computer Vision and Image Analysis*, p. 321, 2005.
- [2] J. B. Jawale and A. S. Bhalchandra, "The Human Identification System Using Multiple Geometrical," *International Journal of Emerging Technology and Advanced Engineering*, vol. 2, no. 3, pp. 662 - 666, 2012.
- [3] T. Dunstone and N. Yager, *Biometric System and Data Analysis: Design, Evaluation, and Data Mining*. Springer, , Eveleigh, NSW 1430: Springer, 2009.
- [4] J. Taliba, "Moment Based Extraction on Handwritten Digits. Doctor Philosophy. University Technology Malaysia, Skudai,," 2005.
- [5] S. A. Daramola and O. D. Oluwaninyo, "Automatic Ear Recognition System using Back Propagation Neural Network," *International Journal of Video & Image Processing and Network Security IJVPNS-IJENS*, vol. 11, no. 01, pp. 28-32, 2011.
- [6] B. S. EL-Desouky, M. El-Kady, M. Z. Rashad and M. M. Eid, "Ear Recognition and Occlusion," *International Journal of Computer Science & Information Technology (IJCSIT)*, vol. 4, no. 6, pp. 97 - 104, 2012.
- [7] A. Hussein and A. Al-Timemy, "A Robust Algorithm for Ear Recognition System Based on Self Organization Maps. The 1st Regional Conference of Eng. Sci. NUCEJ,," vol. 11, pp. 315-321, 2008.
- [8] Y. Xu and W. Zeng , "Ear Recognition Based on Centroid and Spindle," *Procedia Engineering*, vol. 29, no. 1, pp. 2162 - 2166, 2012.
- [9] H. M. El-Bakry and N. Mastorakis, "Ear Recognition by using Neural Networks," *Mathematical Methods and Applied Computing*, pp. 770-804, 2005.
- [10] N. Jamil, A. Almisreb and A. A. Halin, "Illumination - Invariant Ear Authentication," *Procedia Computer Science*, vol. 42, pp. 271 - 278, 2014.
- [11] A. S. Anwar, K. K. A.Ghany and H. Elmahdy, "Human Ear Recognition Using Geometrical Features Extraction," *Procedia Computer Science*, vol. 65, pp. 529 - 537, 2015.
- [12] Z. Huang and J. Leng, "Analysis of Hu's Moment Invariants on Image Scalling and Rotation," in *Conference on Computer Engineering and Technology*, China, 2012.
- [13] D. Shailaja and P. Gupta, "A Simple Geometric Approach for Ear Recognition," in *9th International Conference on Information Technology (ICIT'06)*, 2006.
- [14] R. Mukundan and K. R. Ramakrishnan, *Moment Functions in Image Analysis Theory and Applications*, Singapore: World Scientific Publishing Co Pte. Ltd, 1998.
- [15] Y. Bin and P. Jia-xiong, "Improvement and Invariance Analysis of Zernike Moments using as a Region-based Shape Descriptor," in *Proceeding XV Brazilian Symposim on Computer Graphics and Image Processing*, IEEE, 2002.
- [16] N. A. Bakar and S. M. Shamsuddin, "United Zernike Invariants for Character Images," pp. 498 - 509, 2009.
- [17] A. Gionis, H. Mannila and P. Tsaparas, "Clustering Aggregation," *ACM Transaction on Knowledge Discovery from data*, vol. 1, no. 1, pp. 1-30, 2007.
- [18] S. M. Guthikonda, "Kohonen Self-Organizing Maps," Wittenberg University, 2005.
- [19] H. Yin, "The Self Organizing Maps: Background, Theories, Extensions and Applications," *Studies in Computational Intelligence (SCI)*, vol. 115, pp. 715 - 762, 2008.

## Authors' information

Computer Science Department, Binus Graduate Program, Bina Nusantara University, Jakarta, Indonesia.

E-mails: [suharjito@binus.edu](mailto:suharjito@binus.edu)  
[alpha.epsilon@binus.edu](mailto:alpha.epsilon@binus.edu)  
[girsang@binus.edu](mailto:girsang@binus.edu)



**Suharjito** is the Head of Information Technology Department in Binus Graduate Program of Binus University. He received under graduated degree in mathematics from The Faculty of Mathematics and Natural Science, GadjahMada University, Yogyakarta, Indonesia in 1994. He received master degree in information technology engineering from Sepuluh November Institute of Technology, Surabaya, Indonesia in 2000. He received the PhD degree in system engineering from the Bogor Agricultural University (IPB), Bogor, Indonesia in 2011. His interest research are intelligent system, Fuzzy system, image processing and software engineering.



**Alpha Epsilon** received his Bachelor degree of Informatics majoring Computer Science from Sriwijaya University, Indonesia in 2014. Presently, he is pursuing the Graduate Program of Information Technology at Bina Nusantara University, Indonesia. His research interest includes Biometric, Java programs and Web Design.



**Abba Suganda Girsang** is currently a lecturer at Master in Computer Science, Bina Nusantara University. He obtained his Ph.D. from the Institute of Computer and Communication Engineering, Department of Electrical Engineering, National Cheng Kung University, Tainan, Taiwan. He got his bachelor from the Department of Electrical Engineering, GadjahMada University (UGM), Yogyakarta, Indonesia, in 2000. He then pursued his master degree in the Department of Computer Science in the same university in 2006–2008. He was a staff consultant programmer in Bethesda Hospital, Yogyakarta, in 2001 and also worked as a web developer in 2002–2003. He then joined the Department of Informatics Engineering in Janabadra University as a lecturer in 2003-2015. His research interests include swarm, intelligence, combinatorial optimization, and decision support system.

## Check 23. Journal IREACO Scopus Human ear recognition methods based on image rotation.pdf

### ORIGINALITY REPORT

5%

SIMILARITY INDEX

2%

INTERNET SOURCES

6%

PUBLICATIONS

2%

STUDENT PAPERS

### PRIMARY SOURCES

1

Submitted to University of Babylon

Student Paper

2%

2

Choraś, Michał. "EAR BIOMETRICS BASED ON GEOMETRICAL FEATURE EXTRACTION", Series in Machine Perception and Artificial Intelligence, 2009.

Publication

1%

3

Supardi, Julian, Intan Anindyana Hapsari, and Maheyzah Md Siraj. "Handwritten alphabets recognition using twelve directional feature extraction and self organizing maps", 2014 International Conference on Computer Control Informatics and Its Applications (IC3INA), 2014.

Publication

1%

4

Fergyanto E. Gunawan, Intan A. Hapsari, Benfano Soewito, Sevenpri Candra. "A study of comparison of feature extraction methods for handwriting recognition", 2016 International Seminar on Intelligent Technology and Its Applications (ISITIA), 2016

1%



---

Exclude quotes	On	Exclude matches	< 1%
Exclude bibliography	On		